Soft Matter

Accepted Manuscript

ROYAL SOCIETY OF CHEMISTRY

www.rsc.org/softmatter

Soft Matter

ARTICLE

Received 00th January 20xx,
Accepted 00th January 20xx
DOI: 10.1039/x0xx00000x
www.rsc.org/

Pseudotannins Self-assembled into Antioxidant Complexes

H. A. Cheng,[a] C. T. Drinnan,[a] N. Pleshko,[a] and O. Z. Fisher[a]*

Natural tannins are attractive as building blocks for biomaterials due to their antioxidant properties and ability to form interpolymer complexes (IPCs) with other macromolecules. One of the major challenges to tannin usage in biomedical applications is their instability at physiological conditions and a lack of control over the purity and reactivity. Herein, we report the synthesis and characterization of tannin-like polymers with controlled architecture, reactivity, and size. These pseudotannins were synthesized by substituting linear dextran chains with gallic, resorcylic, and protocatechuic pendant groups to mimic the structure of natural hydrolysable tannins. We demonstrate that these novel materials can self-assemble to form reductive and colloidally stable nanoscale and microscale particles. Specifically, the synthesis, turbidity, particle size, antioxidant power, and cell uptake of IPCs derived from pseudotannins and poly(ethylene glycol) was evaluated.

Introduction

Tannins are a class of abundant and naturally occurring macromolecular polyphenols commonly consumed in the human diet. Their ability to self-assembly with other water soluble macromolecules makes them potentially useful as building blocks for biomaterials. Certain natural tannins are also known to possess medicinal properties which may be better exploited or enhanced in combination with drug delivery technology. Naturally derived tannins are a limited resource and can be difficult to extract from plant sources with the purity required for pharmaceutical and other biomedical applications. Here we describe the synthesis and characterization of tannin-like polymers capable of self-assembling into nanoscale and microscale colloids with redox-responsiveness.

Historically, the term 'tannin' has referred to any polyphenolic compound capable of producing leather from animal skin, or more broadly to polyphenols of sufficient size and aqueous solubility to form intermolecular polymer complexes (IPCs) with proteins.[1] They are often consumed in the human diet as components of plants to which they provide structural integrity and a defense against herbivores.[2, 3] Tannins appear to act as a deterrent to predation in part by readily forming ICs with digestive enzymes in the gastrointestinal tract, thereby limiting nutrient absorption. This interaction has also been shown to occur between natural tannins and synthetic polymers such as poly(ethylene glycol) (PEG)[4-7]. Self-assembly with PEG is particularly useful due to its uniquely high biocompatibility and wide use in the design of bioengineering technology. Natural tannins have proven useful as anti-diabetic agents[8-10], anti-cancer agents[9, 11], antiviral agents[12], and therapeutic antioxidants[11, 13]. This suggests that biomedical devices that incorporate tannins may be imbued with similar properties.

Tannic acid (TA), an extract of chinese gallnuts, has recently been evaluated in the design of several biomaterials as an integral component.[7, 14-19] Kim and coworkers[14] successfully designed pH-responsive multilayers of doxorubicin loaded micelles using alternating layers of TA and micelles constructed from a PE derived amphiphile. Schmidt and Hammond[15] engineered electrochemically removable thin films using layer-by-lay deposition (LbL) of TA and poly(vinylpyrrolidone) (PVPON) in alternating layers. Here, the presence of phenolic hydroxyl groups on TA provided strong hydrogen bonding for material integrity and weak acidity for pH-responsiveness. TA/PVPON films could be removed from an electrode surface by locally increasing the pH through the electrochemical reduction of oxygen. Shutava and coworkers[19] developed pH-responsive drug loaded capsules by incorporating TA into capsule walls. Negatively charged phenoxide groups on TA allow it to form polyelectrolyte complexes with polycations. These complexes displayed accelerated decomposition at both high (>7) and low (<5) pH. The galloyl units on TA provide it with potentially therapeutic antioxidant power. This was exploited in the design of poly(tannic acid) microparticles capable of free radical scavenging by Sahiner and coworkers.[18]

A major challenge to working with TA in biomedical applications is instability above neutral pH.[20] TA can be structurally categorized as hydrolyzable tannin. It consists of depsidic bonds linking together branched galloyl moieties that radiate out from a central glucose core (**Figure 1**). These depsidic bonds readily hydrolyze at physiological pH. It has been shown that IPCs containing TA and certain polymers are hydrolytically stable at basic pH values. Erel Unal and Sukhishvili[7] evaluated neutral polymers, including PEG, as complexation partners with TA in LbL films for stability across pH values. Hydrogen bonded films could be fabricated at pH 2 and were shown to be stable up to pH 8. Such materials can be used as drug delivery vehicles for therapeutic compounds. For example, Shukla and coworkers[17] formed H-bonded multilayer coating using alternating layers of TA and thrombin that could be used to stop uncontrolled bleeding.

One of the major difficulties in working with vegetable tannins is that they are primarily available as impure plant extracts with little control over the size or chemical structure. It is also difficult to obtain natural polyphenols of sufficiently high molar mass to study the dynamics of IC formation. The investigation of vegetable tannins as tanning agents has been limited to a narrow range of

[a] Department of Bioengineering, Temple University, 1947 N 12th Street, Philadelphia, PA.
*Corresponding Author: ozf@temple.edu.
Electronic Supplementary Information (ESI) available: [details of any supplementary information available should be included here]. See DOI: 10.1039/x0xx00000x

molar masss from 0.5 to 3 kDa.[1] There is also a limited variety of tannins that are commercially available. The compounds described in this work were inspired in part by the structure of 1, 2, 3, 4, 6-penta-O-galloyl-β-D-glucose (PGG), one of the simplest hydrolysable tannins. PGG is similar in structure to TA but composed of only non-depsidic ester linkages[8]. A method for the synthetic production of PGG was described by Khanbabaee and Lotzerich.[21] This method was adapted by replacing the central glucose core with a polysaccharide of controlled size (**Figure 1**). In this way, we were able to create pseudotannins across a range of sizes. In addition to galloyl esters, we also investigated resorcinolic and catecholic pendant groups which are commonly found in the structure of condensed tannins. PEG was evaluated as a complexation partner for these compounds towards the goal of engineering self-assembling biocompatible polymer nanoparticles.

Polymeric nanoparticles have a wide range of applications, particularly in bioengineering and biomedical applications.[22, 23] Drug loaded and stimuli-responsive nanoparticles represent a uniquely non-invasive means for diagnosis and treatment of various conditions and microenvironments in the body. The increased surface area and potential for specific targeting can significantly improve the efficacy of any drug and biologic loaded into the nanoparticle. Instead of doping particle formulations with a stimuli responsive agent there has been significant interest in incorporating biological activity into the polymers themselves making the nanoparticles inherently bioactive. This includes polymers that are sensitive to changes in temperature, pH, enzyme activity, and radiation. Of particular interest for targeting disease sites is oxidation responsiveness. Oxidation is a ubiquitous biological mechanism associated with various conditions and diseases and is an important part of both immunological and healing pathways. Elevated levels of oxidation can be associated with various conditions related to autoimmune, neurodegenerative, and cardiovascular diseases. A nanoparticle that responds to oxidation could both target and mitigate those oxidative sites. Here, we describe the synthesis and characterization of tannin-like polymers with controlled architecture, reactivity, and size that were used to self-assemble polymeric nanoparticles. A model of physiological oxidative stress was used to quantify the redox-responsive of pseudotannin derived IPCs and assess any relationship between redox activity and polymer size or architecture.

Experimental Section

Materials

N,N'-Diisopropylcarbodiimide (DIC), 4-dimethylamino-pyridine (DMAP), dimethyl sulfoxide (DMSO), dichloromethane (DCM), dimethylformamide (DMF), Pd black, lipopolysaccharide (LPS), Hoechst-3342, sodium ascorbate, sodium carbonate (Na_2CO_3), Folin & Ciocalteu's phenol reagent, PEGs, nitroblue tetrazolium salt (NBT), xanthine oxidase (XOD), hypoxanthine monosodium salt (HX), and dextrans were purchased from Sigma Aldrich. TBBA and 35BBA were purchased from Tokyo Chemical Industry. 34BBA was purchased from Ubi-Chem. MDA-MB-231 (human breast cancer cells) and J774.2 (mouse leukemia cells) cell lines were purchased from ATCC. RPMI-1640 was purchased from Lonza. Fetal bovine serum (FBS) was purchased from Gemini Bio-Products. Hank's Balanced Salt Solution (HBSS) was purchased from HyClone. Penicillin, streptomycin, amphotericin B, Texas Red sulfonyl chloride, sodium pyruvate, trypsin-EDTA, and GlutaMAX™ were purchased from Life Technologies. 3-3'-Dioctadecyloxacarbocyanine perchlorate (DiO) was purchased from Santa Cruz Biotechnology, Inc. CellTiter 96® AQ_{ueous} Non-Radioactive Cell Proliferation Assay (MTS) was purchased from Promega.

Pseudotannin Synthesis

Pseudotannin synthesis involved two main steps. The first step was the esterification of hydroxyl groups on dextran with 34BBA, 35BBA, or TBBA at a 1:1 COOH-to-OH ratio. In a typical reaction, a solution of TBBA (0.83 g, 1.88 mmoles), dextran (0.1 g), DMAP (0.23g, 1.88 mmoles), and DIC (0.238 g, 1.88 mmoles) in a 2:5 DCM/DMSO mixture is reacted for 72 h at RT. The gum-like product was precipitated in 0.15M HCl, separated by centrifugation at 17,000 rcf, and redissolved in 10 mL DMF. This process was repeated 5x. The product was then deprotected over Pd black under H_2 (balloon pressure) at 40ºC for 72 hours. The deprotected product was filtered through cotton, sand, celite, and finally passed through a 0.45µm PTFE filter. Solvent was then removed via rotary evaporation. The viscous oily product was then dissolved in 2.0M aq Na_2CO_3 followed by dialysis (2000 molar mass cut-off) against 5mM aq sodium ascorbate for two days. The ascorbate solution was changed daily A final dialysis against pure water was done prior to lyophilization. The resulting dry powders were stored under nitrogen at -20°C as polyphenoxide sodium salts. The deprotection step was confirmed by ^{1}H NMR with a 300 MHz Varian spectrophotometer.

Fourier Transform Infrared (FT-IR) Spectroscopy

Pseudotannin samples were taken immediately after deprotection and 20µL was smeared onto barium fluoride (BaF_2) windows. The windows were then washed in acetone and air dried prior to imaging on a Spotlight 400 FTIR Imaging System (PerkinElmer Inc., Waltham, MA). The spectral data were collected in transmittance mode with 32 co-added scans at an 8 cm^{-1} resolution from 750 to 2000 cm^{-1}, and converted to absorbance. To identify peaks that underlie the broad absorbance bands, second derivative spectra were calculated by application of a 15 point smooth Savitsy Golay processing algorithm. Negative peaks of the second derivative spectra of each sample were identified in the fingerprint region (1800 - 800 cm^{-1}).

IPC Formulation

IPCs were formed by first mixing aqueous solutions of PEG and polyphenoxides up to 90% of the desired volume. Then, 10 vol% 1M aq sodium phosphate, pH 7.4, was added to induce complexation. The mixtures were allowed to complex for 1 hour. By changing the ratio of PEG to polyphenoxide, or the molar mass of PEG, the size of IPCs could be tailored to microscale or nanoscale. The turbidity of the resulting colloids was analyzed with UV-Vis spectroscopy by measuring the absorbance of each sample at 550nm using an Infinite® M200 microplate reader (Tecan Group Ltd.). Prior to turbidity measurements, the absorbance of the colloids from 400-800

nm was measured to confirm no specific absorbance peaks in the visible spectrum.

Folin Ciocalteu Assay

The antioxidant potential of IPCs was measured relative to a gallic acid standard as previously described[24]. Specifically, a volume of 60 µL of IPC colloid and 10 µL Folin & Ciocalteu's phenol reagent were combined in microplate wells. After 8 minutes of incubation, 180 µL of 0.36M Na_2CO_3 was added to each well and incubated for an additional 1 hour. The absorbance of each sample at 750nm was then measured using a microplate reader.

Superoxide Scavenging Assay

The NBT oxidation inhibition assay was conducted in 96-well microplates. Specifically, 200 µL of IPC colloid in 0.1 M sodium phosphate buffer at pH 7.4 was prepared in each well. Colloids were complexed for one hour before use with or without 300 kDa linear PEG. Control samples were composed of phosphate buffer alone. Then 20 µL of 30 mM aq HX and 20 µL NBT dissolved in 70% DMF/H_2O was mixed into each well. To this mixture at 25 °C, 20 µL of XOD (0.015 units) was added, and the absorbance at 560 nm was recorded at 0 and 5 minutes. The rate of conversion was calculated as the change in absorbance over this period. The % NBT oxidation inhibition was calculates as 100 x (rate of control – rate of sample)/(rate of control).

Cell Viability

MDA-MB-231 and J774.2 cells were maintained in standard conditions as suggested by the manufacturer. Maintenance media for MDA-MB-231 cells consisted of RPMI-1640 with 10% FBS, 1% GlutaMAX™, 100 U/mL of penicillin, 100 µg/mL of streptomycin, and 250 ng/mL amphotericin B. Maintenance media for J774.2 cells was same with the addition of 1 mM sodium pyruvate. J774.2 cells were gently scraped, collected, and seeded into individual wells of a 96-well plate at 50,000 cells/well. MDA-MB-231 cells were enzymatically removed from flasks with 0.25% Trypsin-EDTA and seeded into individual wells at 100,000 cells/well. Seeding media consisted of maintenance media without antibiotics or antimycotics and with HI-FBS used in lieu of FBS. Cells were allowed to attach overnight. Phagocytic activity of J774.2 was promoted with 1 µg/ml of LPS during cells attachment. Microparticles composed of gallol, catechol, and resorcinol modified, 6 kDa dextran were formed with linear, 20 kDa PEG over 1 hour as described previously. Cells were exposed to various concentrations in seeding media over 1 day, and viability was assessed with a commercial MTS assay using standard conditions. Briefly, cells were washed 3X with HBSS and exposed to the prepared MTS reagent for 2 hours. Absorbance was measured at 490 nm using a Tecan Infinite® 200 Pro and normalized to cells not exposed to microparticles (control).

Cell Uptake. To visualize phagocytic uptake, fluorophore tagged microscale IPCs were formed. To make a fluorescent PEG derivative, a 40 kDa 8-arm amine terminated PEG (JenKem Technology) at a 1:8 mole ratio with Texas Red sulfonyl chloride was allowed to react in DMSO with a 3-fold molar excess of TEA overnight at RT. The product was purified by dialysis and lyophilized to obtain a purple powder. To make microscale fluorescence IPCs, a mixture of 1% 8-arm PEG-Texas Red and 99% linear 20 kDa PEG was complexed with polyphenoxide derived from 6 kDa dextran at a 3:1 mass ratio and 3.6 mg/mL total polymer concentration. The complexation was allowed to proceed in 0.1M sodium phosphate buffer for one hour in the dark before uptake studies.

J774.2 and MDA-MB-231 cells were seeded at 100,000 and 200,000 cells, respectively, in chambers of an 8-well chamber slide (Nunc™ Lab-Tek™ II Chamber Slide™ System) along with phenol free media. Cells were allowed to attach overnight and phagocytic activity of J774.2 cells was promoted with 1 µg/mL of LPS. Cells were exposed to Texas Red loaded IPCs for 6 hours and visualized with a laser scanning confocal microscope (Olympus Corp.). J774.2 cells were pretreated with DiO to stain cellular membranes. Nuclei were counterstained with Hoechst-33342 and cells were fixed for 10 min with 10% formalin in DPBS.

Statistical Analysis

All data is expressed as mean ± standard deviation (SD), where applicable. The student's T-test was used to identify significant statistical differences ($p<0.05$).

Results and Discussion

Pseudotannin Synthesis

Dextran was used as an analogue to the carbohydrate core of natural hydrolysable tannins to make pseudotannins with controllable shape and molar mass (**Figure 1**).[25] Dextrans are commonly used as standards for gel permeation chromatography and can therefore be procured in a wide range of molar masss with low polydispersity. The biodegradability of dextran may prove beneficial in the future clinical use of pseudotannins. The reaction scheme used in this work may also work using other polysaccharides. Pseudotannins were synthesized with gallol, catechol, and resorcinol residues using benzyl protected precursors 3,4,5-tris(benzyloxy)benzoic acid (TBBA), 3,4-bis(benzyloxy)benzoic acid (34BBA), and 3,5-bis(benzyloxy)benzoic acid (35BBA) respectively. The phenolic residues were chosen because of their presence on naturally occurring tannins. The conjugation of each to the dextran was based on the esterification reaction described previously[21] with modifications[25]. **Figure 2** illustrates the reaction scheme for the esterification and deprotection steps using polygallol as an example. Proton nuclear magnetic resonance was used to confirm full deprotection by the lack of -CH_2O- shifts at 5.0 and 5.1 ppm as previously described.[26] (**Supplemental Figures 1-3**). The resulting pseudotannins were immiscible in water. A carbonate buffer was used to solubilize the compounds and ease purification. Attempts to determine the molar mass and molar mass distributions for the polymer conjugates using gel permeation chromatography and mass spectroscopy were unsuccessful as previously reported (data not shown).[25]

FT-IR Spectroscopy

The IR spectra of each pseudotannin (**Supplemental Table 1, Supplemental Figure 4**) presented unique peaks in the fingerprint region (800 to 1800 cm^{-1}). The second derivative spectrum (**Supplemental Figure 5**) shows distinct, narrower negative

absorbance peaks in the fingerprint region. Peaks from 1590-1700 cm^{-1} were attributed to C=O stretching in the ester bonds.[27, 28] Peaks from 1415-1570 cm^{-1} were attributed to C=C stretching in the aromatic rings.[28] Peaks from 1003-1390 cm^{-1} were attributed to a combination of C-O stretching[29] and in-plane aromatic C-H bending[28]. Peaks from 750-900 cm^{-1} were attributed to out-of-plane aromatic C-H bending.[28] As expected, the IR spectrum for polygallols had a combination of peaks present both in resorcinol (1480cm^{-1} and 1600cm^{-1}) and catechol (1360cm^{-1} and 1520cm^{-1}) spectra. Each class of pseudotannin was uniquely identifiable. There are several distinct peaks (1712, 1658, 1600, 1438, 1411, 1384, 1157, 1122, and 1099, 930cm^{-1}) conserved among the three classes of pseudotannin, and a number of these (1330, 1122, and 930 cm^{-1}) correspond with major peaks in dextran.[30] There are also several negative peaks that form unique signatures for each formulation. Distinct peaks at 883, 1014, and 1361 are unique to the polycatechol samples. A cluster of peaks from 1022-1072 cm^{-1}, distinct peaks at 852 and 1002cm^{-1}, and a lack of a distinct peak at 1530 are unique to the polyresorcinol samples. A cluster of peaks from 1349-1187cm^{-1}, including a lack of a distinct peak at 1292, 1300, and 1340, distinct peaks at 871 and 1036cm^{-1} are unique to the polygallol samples.

Turbidity and Polycomplex Stability

The plurality of hydrogen bond donating groups on the pseudotannins allow for the self-assembly of IPCs with PEG in solution. Before complexation was allowed to proceed, aqueous solutions of PEG and polyphenoxides were mixed together. Then phosphate buffer was added to achieve a final concentration of 0.1 M sodium phosphate and pH 7.5, and an IPC concentration below 0.5 mg/mL. The phosphate acted as a hydrogen source for the protonation of polyphenoxides. This caused their immediate precipitation or colloidal complexation depending on the amount of PEG used. Formulating IPCs at higher concentrations generally resulted in unstable colloids.

Turbidity studies were used to to understand the important parameters for achieving both complex and colloidal stability. Polycomplexation between polyacids and PEG was given a theoretical treatment by Baranovsky and colleagues[31] which provided a framework understanding the interaction between our pseudotannins and PEG in solution. The stability of polycomplexes is known to depend on polymer molar mass[31] and branching[32]. Generally, a PEG/polyphenoxide mass ratio above 1 was enough to achieve colloidal stability (the absence of visible sedimentation). A range of PEGs with varying molar mass and branching were evaluated. Representative data is shown in **Figure 3**. A parabolic relationship was observed between turbidity values and PEG MW when pseudotannin size and mass ratio were held constant (**Figure 3A**). This relationship was consistent for all three classes of pseudotannin and independent of the mass ratio of the two polymers. The increase in turbidity with molar mass is similar to the relationship Baranovsky and coworkers[31] described between complex stability and molar mass. A sharp change in turbidity was observed when 100 kDa PEG was used. When viewed under the microscope the polycomplexes with the lowest PEG molar masss either showed diffuse precipitate or spherical microstructures. These spherical microstructures appeared smaller as the PEG length increased. Samples made with 100 kDa PEG contained no visible particulates when viewed under the microscope. Dynamic light scattering confirmed that these samples contained colloidal particles less than a micron in diameter. Unexpectedly, the MW of the pseudotannins appeared to affect turbidity much less than that of PEG (**Figure 3B**). This may be due to the inability of larger pseudotannins to form extended ladder-type assemblies with PEG before intramolecular bonding dominates. The initial step in IPC formation linear ladder-type bridging between polymers such as those observed in the complexation of complementary strands of oligonucleotides.[33] The ladder-type model assumes both complexation partners are fully solvated. The insolubility of the pseudotannins in water deviates from that model. A drop in turbidity as a function of branching was observed when pseudotannins were complexed with multi-arm PEGs as shown in **Figure 3C**. Branching has previously been shown to weaken complex stability.[32]

Dynamic Light Scattering

Dynamic light scattering was used to analyze average particle diameters of IPC solutions. **Table 1** shows the average particle diameter of IPC formed from pseudotannins derived from 6 kDa dextran and 300 kDa PEG. The polygallol IPCs formed the largest particles with an average diameter of 241 nm. Polyresorcinol and polycatechol IPCs formed 179 nm and 158 nm particles respectively. These sizes are small enough for endocytosis into mammalian cells.[34]

Folin-Ciocalteu Assay

The Folin-Ciocalteu method is commonly used to determine the phenolic or antioxidant content of polyphenol extracts from natural sources.[24] We used the method to determine the phenolic content of the pseudotannins and the respective IPCs that they form. **Figure 4** shows the antioxidant potential of IPCs as a function of type of pseudotannin, mass ratio, and MW of pseudotannin. **Figure 4A** shows that 6kDa gallic complexes had the highest antioxidant potential. **Figure 4B** showed that for a standard amount of a pseudotannin, a higher PEG-to-pseudotannin ratio resulted in an apparent greater antioxidant potential. It appears that as this ratio increased, PEG increased the availability of the pseudotannin pendant groups to the Folin-Ciocalteu reagent. This suggests that increasing the PEG content of IPCs enhances colloidal stability while weakening complex stability. Weaker complexes would allow for greater interaction with solvent and other solutes. **Figure 4C** shows that IPCs with made with lower molar mass pseudotannins show a higher antioxidant potential as measured by the Folin Assay. This suggests that the complexes made with higher molar mass pseudotannin are more stable and trap more of the phenol groups within the complex, exposing fewer phenolic groups to the Folin-Ciocalteu reagent.

Superoxide Scavenging Assay

While the Folin-Ciocalteu assay provides a useful measure of antioxidant power, it does not indicate responsiveness to physiological oxidation. To characterize their ability to scavenge superoxide, an NBT oxidation inhibition assay was conducted on pseudotannin complexes with and without PEG, using XOD and HX to generate superoxide. (**Figure 5)** Superoxide is produced extracellular by neutrophils at sites of inflammation and in the phagosome of macrophages. NBT is oxidized to a blue colored formazan in the presence of superoxide. A reduction in the rate of this conversion is proportional to the superoxide radical scavenging

ability of a compound.[35] The results show that polygallols are superior superoxide scavengers when compared to polycatechols and polyresorcinols. Polycatechols showed some superoxide scavenging while polyresorcinols showed very little. Polygallol made from a 6 kDa dextran displayed similar superoxide scavenging ability as homocomplexes and when complexed with 300 kDa PEG (**Figure 5A**). When a larger dextran core was used, the superoxide scavenging ability of polygallols increased significantly when complexed with PEG as compared to homocomplexes (**Figure 5B and 5C**). At all sizes, polycatechols displayed a significant decrease in superoxide scavenging when complexed with 300 kDa PEG at a 1:1 mass ratio compared to homocomplexes. The scavenging ability returned at mass ratios of 5:1 and 10:1.

Cell Viability

The cytotoxicitiy of the pseudotannin/PEG IPCs was evaluated by measuring cell viability after exposure to IPCs for 24 hours. Phagocytic activity in J774.2 cells was promoted with a 1 day pretreatment of phorbol 12-myristate 13-acetate (PMA) before the assessment of cell viability. Cells were exposed to IPCs made with 20 kDa PEG at 3:1 PEG/polyphenoxide mass ratio at a range of concentrations. Viability was assessed using an MTS assay[36].(**Figure 6**) Particle concentration was calculated as total polymer weight per unit volume. This concentration is an overestimate based on the mass of polyphenoxide used in the IPC formulation. The protonation of these polymers would result in lower molar mass polyphenols. **Figure 6** shows that there were no significant decreases in the MTS signal of either cell line except at the highest particle concentration (1mg/mL).). It is important to note that untreated J774.2 cells are slightly phagocytic, but the rate of uptake is increased after exposure to PMA. It is possible that the phenolic content of the IPCs altered NADPH flux inside the cell, thereby affecting the metabolic activity as measured by the MTS assay. This would account for the difference in cell viability between treated and untreated J774.2 cells as shown in **Figure 6A.** Polyphenols have been known to skew the measured viability of cells when a tetrazolium salt-based assay is used.[37, 38] If pseudotannin IPCs are causing this effect, then the data suggests that cell uptake is required for it to occur.

The lowest MTS measurement observed among any of the samples was above the median lethal dose (LD_{50}), demonstrating that the IPCs, as formed, were highly cytocompatible. This was expected, as the IPCs were formed with an excess of PEG by weight, and PEG is known to be cytocompatible.[39, 40] Interestingly, some polycatechol-derived IPCs seem to significantly improve viability or metabolic activity of the non-phagocytic cells. These MTS values were significantly different from those of cells not exposed to microparticles. A determination of the mechanism or cause of the increased cell viability requires further testing.

Phagocytic Uptake

Microscale IPCs for cell uptake were formulated from a 40 kDa 8 arm-PEG Texas Red, a 40 kDa carboxy terminated 8-arm PEG, and polygallol pseudotannin derived from 6 kDa dextran. Here, polycomplexation was used to design particles with just two types of PEG, one being a PEGylated fluorophore. But this method could be expanded to design IPCs which display a larger variety of PEGylated surface moieties, such as ligands for cell uptake, or loaded with combinations of PEGylated drugs or diagnostic imaging agents. This method may be useful for high throughput and combinatorial screening. The uptake of microscale particles by phagocytes can be exploited to deliver therapeutic compounds intracellularly or as an adjuvant to vaccine delivery.[41, 42] Laser scanning confocal fluorescence microscopy confirmed that microscale IPCs had sufficient integrity to be uptaken by phagocytosis. (**Figure 6C-6E**) Fluorescent particles were exposed to mouse macrophages (J774.2) and human breast cancer epithelial cells (MDA-MB-231) for 6 hours before imaging. The phagocytic activity of J774.2 cells was promoted with LPS for 1 day prior to microparticle addition. (**Figure 6D**) MDA-MB-231 cells were used as a non-phagocytic control. (**Figure 6E)** The nuclei were counterstained with Hoechst 33342 (blue) and the membrane was stained prior to microparticle treatment with DiO (green). The LSCM images show the uptake of fluorescent IPCs into phagocytic cells but not non-phagocytic cells.

Conclusions

Taking inspiration from nature, tannin-like polymer conjugates were synthesized with significant control over the structure of phenolic residues and polymer size. Natural tannins have been widely investigated with the intent to control purity and structure, understand self-assembly with macromolecules, enhance the quality of agricultural products, and exploit therapeutic potential. To our knowledge, this preliminary study is the first attempt to synthesize tannin-like compounds and utilize them in the directed self-assembly of microscale and nanoscale biomaterials. Furthermore, this pursuit resulted in the discovery of pseudotannin derived complexes that respond to physiological oxidative stress and can be uptaken by phagocytic cells. Further work is needed to characterize the molar mass and weight distribution of pseudotannins to better understand a correlation between tannin size and function. The dynamics of IPC uptake by phagocytes and their intracellular fate requires further study as well as an *in vivo* evaluation of biocompatibility.

Acknowledgements

The authors thank Mugda Padalkar for assistance with FT-IR spectroscopy experiments, Dr. Charles Debrosse and Gerald Pawlish for assistance with NMR spectroscopy, Dr. Mohammad F. Kiani for assistance with dynamic light scattering measurements, Elaine Minsun Sun, Vincent Zhao, Silvia Lopez, Thomas V. Collins, and Huai-yu Peter Cheng for assistance with synthesis and polymer characterization. This work was supported by a grant from the National Institutes of Health (Grant No. 1R21EB017504 to O.Z.F.) and start-up funds from the Temple University Department of Bioengineering.

References

1. T. White, *Journal of the Science of Food and Agriculture*, 1957, **8**, 377-385.
2. A. Pizzi and F. A. Cameron, *Wood Science and Technology*, 1986, **20**, 119-124.
3. P. D. Coley, J. P. Bryant and F. S. Chapin, *Science*, 1985, **230**, 895-899.

4. D. E. Jones, *Nature*, 1965, **206**, 299-300.
5. H. P. S. Makkar, M. Blummel and K. Becker, *British Journal of Nutrition*, 1995, **73**, 897-913.
6. A. M. Badran and D. E. Jones, *Nature*, 1965, **206**, 622-624.
7. I. Erel-Unal and S. A. Sukhishvili, *Macromolecules*, 2008, **41**, 3962-3970.
8. J. H. Zhang, L. Li, S. H. Kim, A. E. Hagerman and J. X. Lu, *Pharmaceutical Research*, 2009, **26**, 2066-2080.
9. X. Q. Liu, J. Kim, Y. S. Li, J. Li, F. Liu and X. Z. Chen, *Journal of Nutrition*, 2005, **135**, 165-171.
10. S. M. C. Souza, L. C. M. Aquino, A. C. M. Jr, M. A. M. Bandeira, M. E. P. Nobre and G. S. B. Viana, *Phytotherapy Research*, 2007, **21**, 220-225.
11. M. Labieniec, T. Gabryelak and G. Falcioni, *Mutation Research-Genetic Toxicology and Environmental Mutagenesis*, 2003, **539**, 19-28.
12. B. U. Reddy, R. Mullick, A. Kumar, G. Sudha, N. Srinivasan and S. Das, *Sci. Rep.*, 2014, **4**.
13. A. E. Hagerman, K. M. Riedl, G. A. Jones, K. N. Sovik, N. T. Ritchard, P. W. Hartzfeld and T. L. Riechel, *Journal of Agricultural and Food Chemistry*, 1998, **46**, 1887-1892.
14. B. S. Kim, H. Lee, Y. H. Min, Z. Poon and P. T. Hammond, *Chemical Communications*, 2009, 4194-4196.
15. D. J. Schmidt and P. T. Hammond, *Chemical Communications*, 2010, **46**, 7358-7360.
16. E. Costa, M. Coelho, L. M. Ilharco, A. Aguiar-Ricardo and P. T. Hammond, *Macromolecules*, 2011, **44**, 612-621.
17. A. Shukla, J. C. Fang, S. Puranam, F. R. Jensen and P. T. Hammond, *Advanced Materials*, 2012, **24**, 492-496.
18. N. Sahiner, S. Sagbas and N. Aktas, *Materials Science and Engineering: C*, 2015, **49**, 824-834.
19. T. Shutava, M. Prouty, D. Kommireddy and Y. Lvov, *Macromolecules*, 2005, **38**, 2850-2858.
20. R. Osawa and T. P. Walsh, *Journal of Agricultural and Food Chemistry*, 1993, **41**, 704-707.
21. K. Khanbabaee and K. Lotzerich, *Tetrahedron*, 1997, **53**, 10725-10732.
22. J. P. Raoa and K. E. Geckeler, *Prog. Polym. Sci.*, 2011, **36**, 887-913.
23. E. Brewer, J. Coleman and A. Lowman, *Journal of Nanomaterials*, 2011.
24. A. K. Atoui, A. Mansouri, G. Boskou and P. Kefalas, *Food chemistry*, 2005, **89**, 27-36.
25. *United States Pat.*, 2013.
26. O. Z. Fisher, B. L. Larson, P. S. Hill, D. Graupner, N.-K. Mai-Thi, N. S. Kehr, L. De Cola, R. Langer and D. G. Anderson, *Advanced Materials*, 2012, **24**, 3032–3036.
27. L. Y. Foo, *Phytochemistry*, 1981, **20**, 1397-1402.
28. K. Fernández and E. Agosin, *Journal of Agricultural and Food Chemistry*, 2007, **55**, 7294-7300.
29. M. G. Albu, M. V. Ghica, M. Giurginca, V. Trandafir, L. Popa and C. Cotrut, 2009.
30. R. G. Zhbankov, S. P. Firsov, E. V. Korolik, P. T. Petrov, M. P. Lapkovski, V. M. Tsarenkov, M. K. Marchewka and H. Ratajczak, *Journal of Molecular Structure*, 2000, **555**, 85-96.
31. V. Y. Baranovsky, A. A. Litmanovich, I. M. Papisov and V. A. Kabanov, *European Polymer Journal*, 1981, **17**, 969-979.
32. V. Y. Baranovsky, S. Shenkov, V. Doseva and G. Borisov, *Journal of Polymer Science Part a-Polymer Chemistry*, 1996, **34**, 2253-2258.
33. V. A. Kabanov and I. M. Papisov, *Polymer Science USSR*, 1979 **21**, 261-307.
34. O. Z. Fisher, A. Khademhosseini, N. A. Peppas, K. H. J. r. B Editors-in-Chief:Â Â , W. C. Robert, C. F. Merton, I. Bernard, J. K. Edward, M. Subhash and V. r. Patrick, in *Encyclopedia of Materials: Science and Technology*, Elsevier, Oxford, 2009, pp. 1 9.
35. T. P. Krishnakantha and B. R. Lokesh, *Indian journal of biochemistry & biophysics*, 1993, **30**, 133-134.
36. K. Berg, L. Zhai, M. Chen, A. Kharazmi and T. C. Owen, *Parasitology research*, 1994, **80**, 235-239.
37. D. Bernhard, W. Schwaiger, R. Crazzolara, I. Tinhofer, R. Kofler and A. Csordas, *Cancer letters*, 2003, **195**, 193-199.
38. P. Wang, S. M. Henning and D. Heber, *PloS one*, 2010, **5**, e10202.
39. K. Knop, R. Hoogenboom, D. Fischer and U. S. Schubert, *Angewandte Chemie*, 2010, **49**, 6288-6308.
40. Y. Ikeda and Y. Nagasaki, *Journal of Applied Polymer Scien* 2014, **49**.
41. B. R. Carrillo-Conde, A. E. Ramer-Tait, M. J. Wannemueh and B. Narasimhan, *Acta biomaterialia*, 2012, **8**, 3618-3628.
42. R. C. Mundargi, V. R. Babu, V. Rangaswamy, P. Patel and T M. Aminabhavi, *Journal of Controlled Release*, 2008, **125**, 193 209.
1

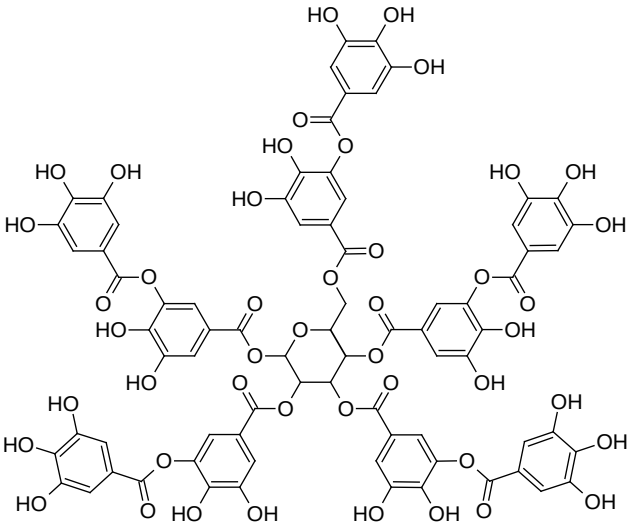

Tannic Acid

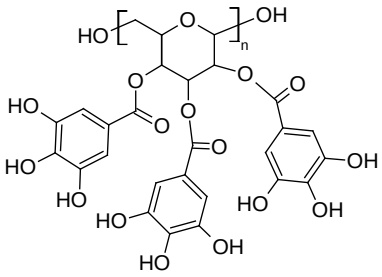

Polygallol

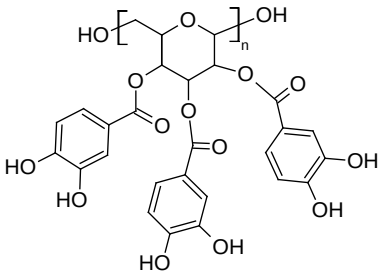

Polycatechol

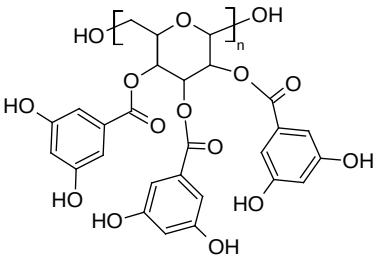

Polyresorcinol

Figure 1. The chemical structure of tannic acid and the theoretical structure of pseudotannins. The structure of tannic acid consists of phenolic units bound to a glucose core via ester bonds. Pseudotannis were designed with a poly(glucose) core (dextran) substituted with phenolic residues via ester bonds. Branching due to α-1,6 glycosidic linkages is left out only for simplicity.

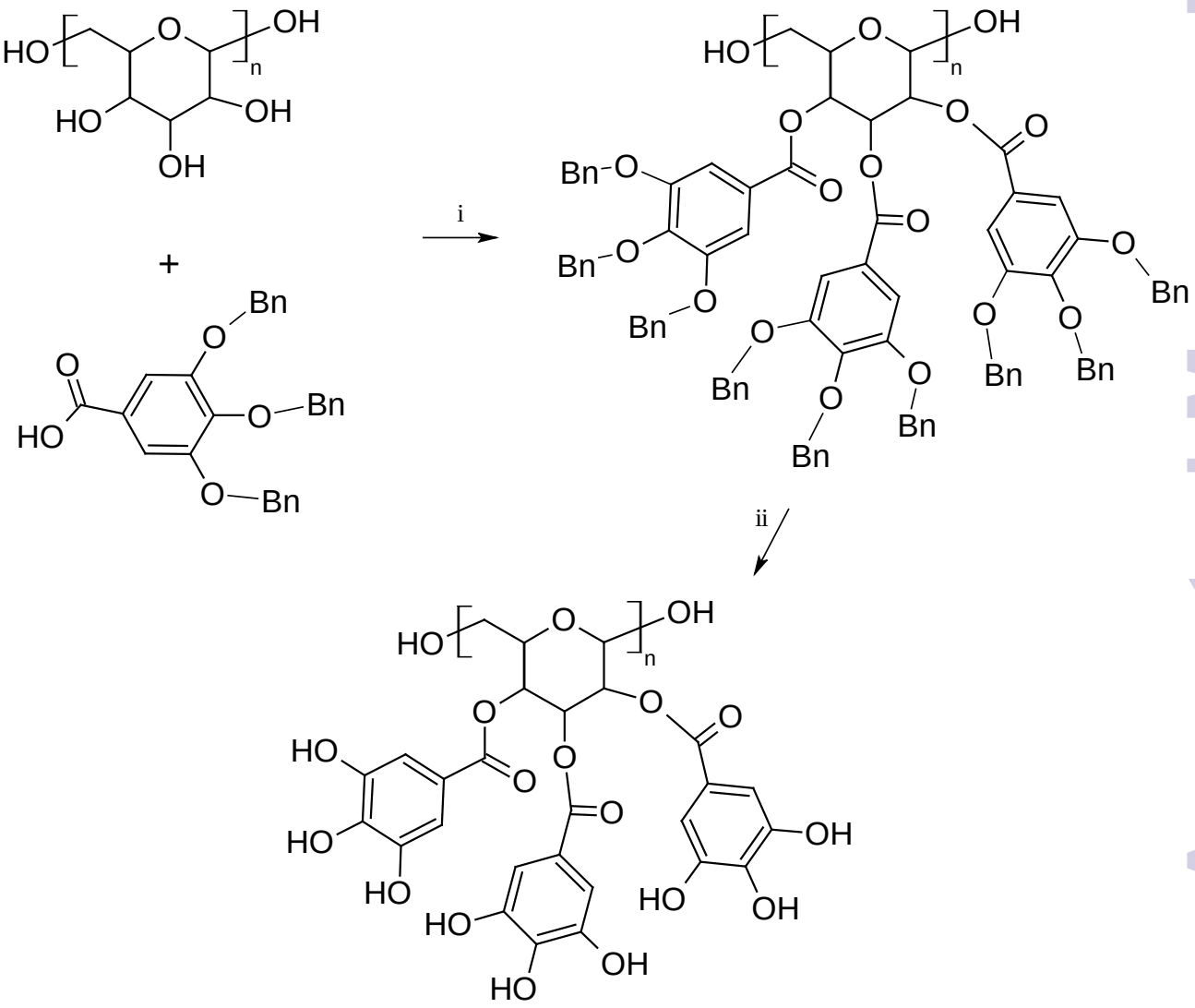

Figure 2. Polygallol pseudotannin synthesis scheme. (i) Benzyl (Bn) protected phenolic residues are reacted with dextran, DIC, and DMAP in DMSO/DCM at room temperature for 72 hours. (ii) The purified product is deprotected over Pd black under H2 in DMF at 40°C for 72 hours. Dextran branching is ignored and polymer end groups are shown as unreacted in this schematic for simplicity.

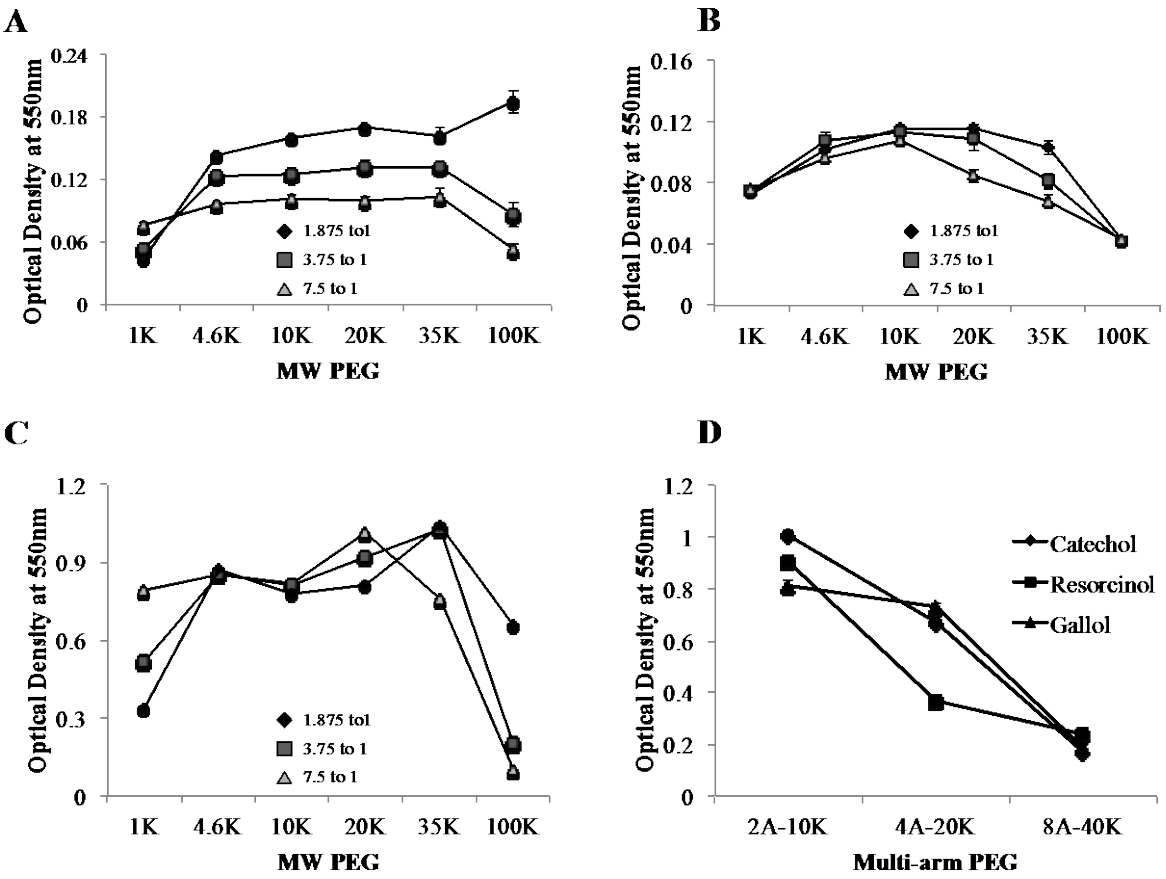

Figure 3. (A-C) Turbidity vs PEG MW of polygallol (A), polyresorcinol (B), and polycatechol (C) IPCs. Linear PEGs were mixed with pseudotannins at mass ratios of 1.875:1 (diamonds), 3.75:1 (squares), and 7.5:1 (triangles). (D) Turbidity of pseudotannin complexes vs PEG branching. Values shown are mean averages of 5 replicates ± standard deviation.

Table 1. Dynamic Light Scattering analysis of IPCs. The average hydrodynamic diameter (n=3) and polydispersity index (PDI) is listed. IPCs were formulated using pseudotannins with 300 kDa PEG at a 5:1 PEG/polyphenoxide mass ratio.

Pseudotannin	Size (nm)	PDI
Gallol	241	0.155
Resorcinol	179	0.255
Catechol	158	0.287

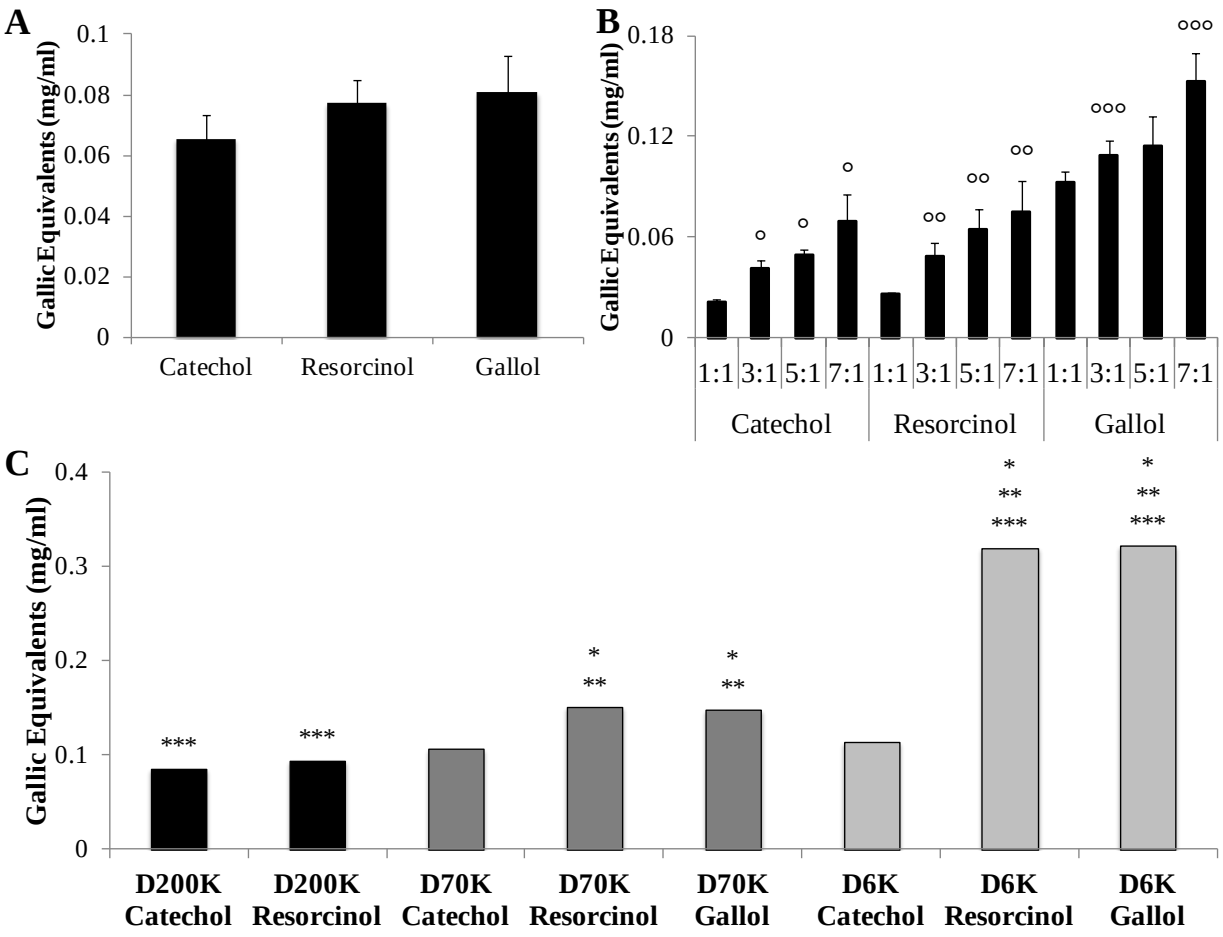

Figure 4. The Folin Ciocalteu assay was used to evaluate the antioxidant potential of IPCs with 20K MW PEG at a 3:1 mass ratio (A). Maintaining a constant mass of pseudotannin and increasing PEG content (B) resulted in an greater apparent antioxidant potential (B).Using a 100 kDa PEG and 5:1 mass ratio, an increase in the size of pseudotannin (D200K represents a 200 kDa dextran core) resulted in an apparent decrease in antioxidant power (C). Values shown are averages of 5 replicates ± standard deviation. °, °°, and °°° represents significant difference (p-value <0.05) when compared to PEG to pseudotannin ratio of 1:1 for polycatechol, polyresorcinol, and polygallol IPCs respectively. *, **, and *** represent significant difference (p-value < 0.05) when compared to D200K, D70K, and D6K catechol IPCs respectively.

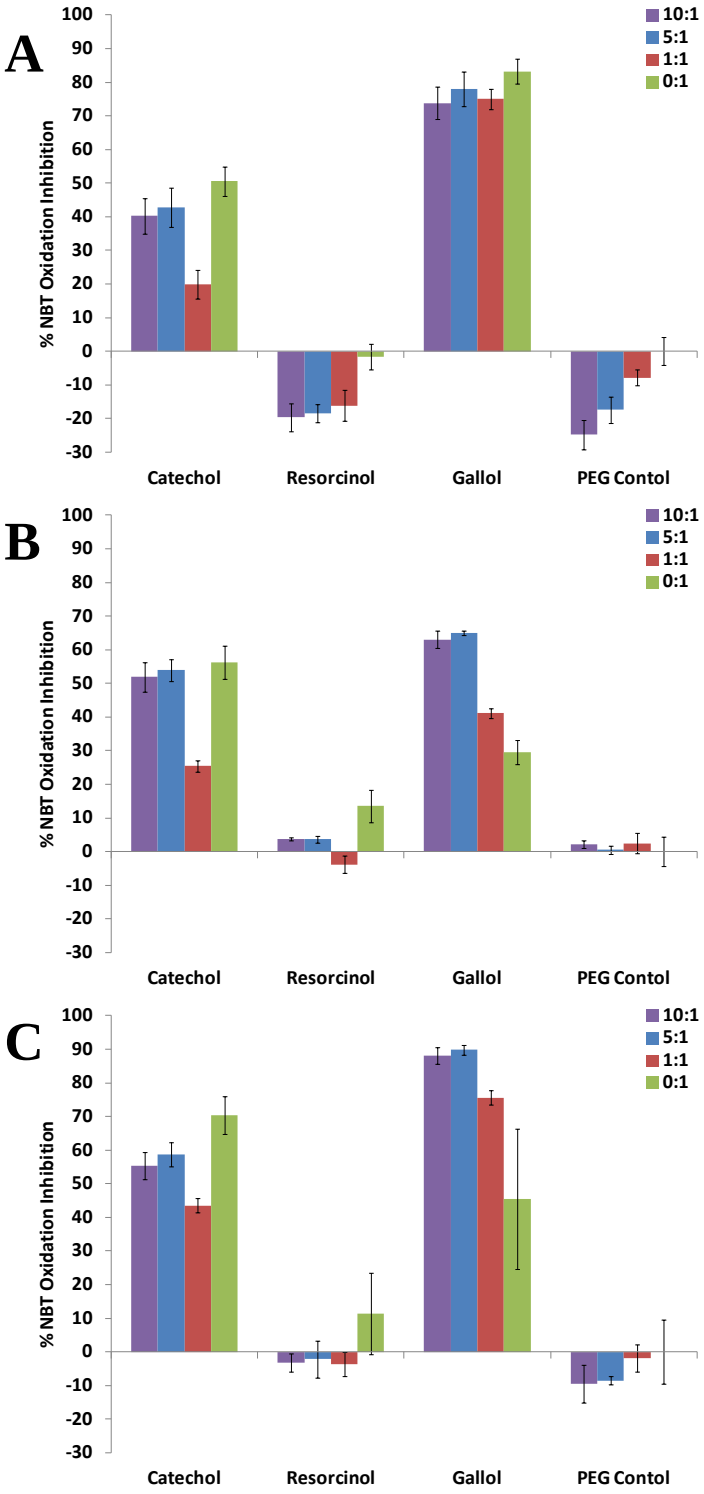

Figure 5. Assay of pseudotannin/PEG complexes, pseudotannin alone, and PEG alone on the rate of conversation of NBT into NBT-diformazan in the presence of superoxide. The legend indicates the mass ratio of 300 kDa PEG to polyphenoxide used in each formulation. The assay was run on pseudotannns derived from 6 kDa dextran (A), 40 kDa dextran (B), and 200 kDa dextran (C). Values shown are averages of 6 replicates ± standard deviation.

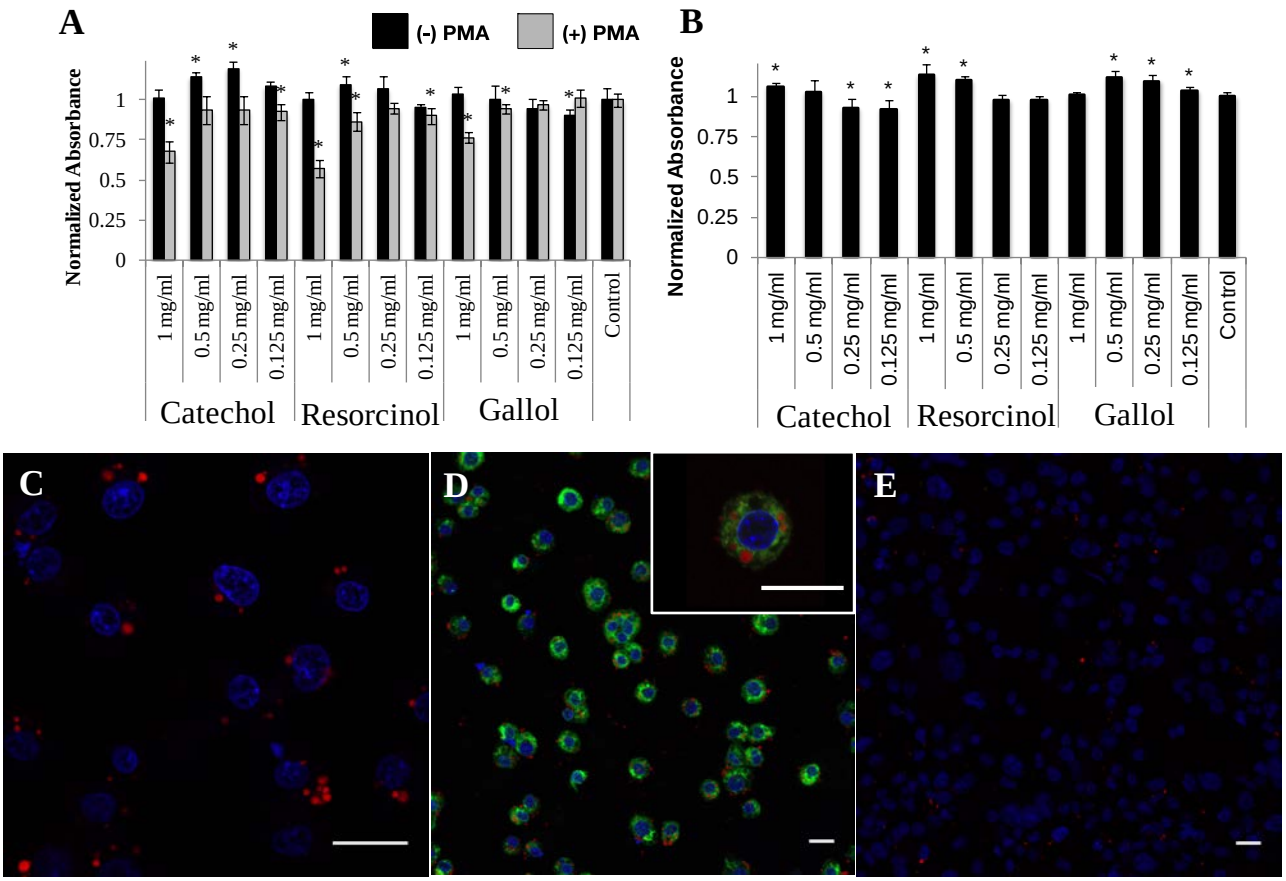

Figure 6. Cell viability and uptake of pseudotannin IPCs. MTS assessment of cell viability (A-B) and LSCM images (C-E) of J774.2 (A,C,D) and MDA-MB-231 (B,E) cells after exposure to fluorescently tagged microscale IPCs. Phagocytic activity was promoted with a 1d pretreatment of PMA (A,C,D). Cell viability was assessed after 1 day exposure of a range of concentrations of PEG/psuedotannin (20 kDa PEG; 3:1 weight ratio) microparticles composed of a variety of psuedotannins. MTS data is normalized to cells not exposed to microparticles. N=5 and data is presented as mean ± standard deviation. * denotes that group is significantly different ($p<0.05$) when compared to cells not exposed to microparticles. J774.2 (C-D) and MDA-MB-231 (E) cells were exposed to Texas Red tagged IPCs for 6 h. MDA-MB-231 (E) cells were used as a non-phagocytic control. Nuclei were counterstained with Hoechst 33342 (blue) and membrane was stained prior to microparticle treatment with DiO (green; B). Scale bars represent 25 µm.

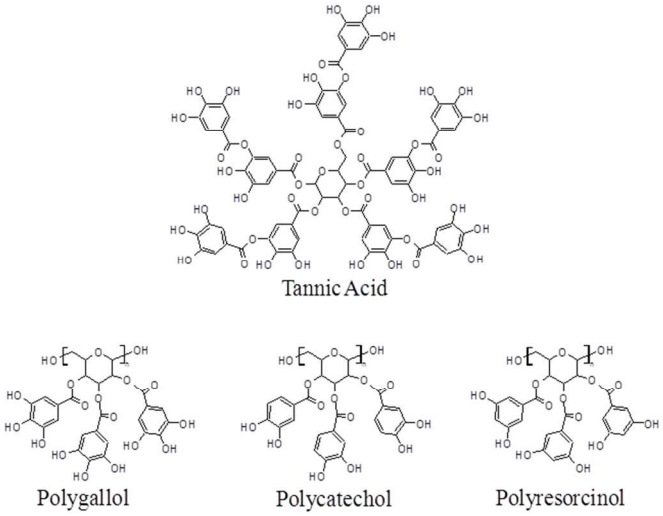

Table of Contents Image. The chemical structure of tannic acid and the theoretical structure of pseudotannins.